ORIGINAL PAPER

Biodegradation and the origin of surface bitumens in the Palaeocene Kolosh Formation, Northern Iraq

Mohamed W. Alkhafaji[1] · Mohamed A. Aljubouri[2] · Falah A. Al-Miamary[3] · Jacques Connan[4]

Abstract

The bitumen from surface exposures of the Palaeocene Kolosh Formation in three areas (Duhok, Shaqlawa and Dokan) of northern Iraq were investigated using GC, GC-MS, carbon and hydrogen isotope ratios of aromatic, NSO and asphaltene to determine their state of alteration (biodegradation, water washing and abiotic oxidation), thermal maturity and potential source rocks. These samples have a high percentage of NSO and asphaltene and minor amounts of saturated and aromatic hydrocarbons. These bitumens have a distinguished biomarker distribution, which can be attributed to different levels of biodegradation. The samples of Group 1 are moderately biodegraded: their normal alkanes and isoprenoids have been removed, whereas their hopanes and steranes are intact or have been very slightly altered. The samples of Group 2 are heavily to very heavily biodegraded; their steranes and hopanes are degraded without the formation of 25-norhopanes. These samples are more oxidized than those of Group 1. The bitumens have different origins, and their terpane and sterane ratios indicate that they were generated by early mature marine carbonate source rocks that were likely to have originated from Jurassic–Lower Cretaceous Formations.

Introduction

The hydrocarbon composition of oil and subsurface bitumen is controlled by many factors, including depositional environments, organic matter sources, thermal maturity levels and alteration processes such as evaporation, biodegradation and water washing (Wang et al. 2016). Alteration processes lead to the creation of tar sand deposits and heavy oil accumulations (Rubinstein et al. 1977), and when bitumen as oil seep is exposed to surface conditions, it undergoes other alteration processes, such as evaporation and abiotic oxidation

✉ Mohamed W. Alkhafaji
Mohamed_wagga@yahoo.com; mohamedajeel@tu.edu.iq

[1] Department of Applied Geology, College of Science, University of Tikrit, Tikrit Iraq

[2] Department of Refining, College of Petroleum and Mining Engineering, University of Mosul, Mosul Iraq

[3] Department of Geology, College of Science, University of Mosul, Mosul Iraq

[4] 23 rue Saint-Exupéry, 64000 Pau France

(oxidation of bitumens by rain waters). External factors, such as oxygen that has been dissolved in rainwater and the action of micro-organisms and atmospheric oxygen, can induce these alteration processes (Charrié-Duhaut et al. 2000). Hydrocarbons are removed during the water-washing process in the following sequence: aromatics, normal alkanes and naphthalenes (Lafargue and Barker 1988), and the solubility of organic compounds increases with increasing temperatures (Lafargue and Barker 1988). However, it is difficult to recognise alterations caused by water washing because biodegradation effects are more pronounced (Wang et al. 2016). When crude oils or bitumen are subjected to microbial degradation, various compounds are removed or altered, depending on their molecular structure, structural configuration and aqueous solubility (Larter et al. 2003). The biodegradation process leads to changes in the properties of oils such as viscosity, API and sulphur content which, in turn, decreases the quality of crude oils (Volkman et al. 1984; Peters and Moldowan 1993; Larter et al. 2012; Lopez et al. 2015). In biodegraded oils, biomarker compounds of the saturate fraction are removed in the following order: normal alkanes, acyclic isoprenoids, regular steranes, hopanes, diasteranes and tricyclic terpanes (Connan 1984; Peters et al. 2005). Crude oils or bitumen contain many biomarkers that are resistant to

biodegradation, such as gammacerane, oleanane, and tricyclic terpanes and are used to assess thermal maturity, sources of organic matter, genetic relationships and levels of biodegradation.

The Palaeocene Kolosh Formation is widespread in northern Iraq and was first described near the town of Koya in High Folded Zone (Jassim and Buday 2006a). It comprises dominantly alternating bedding of blue and black calcareous shale and marl, and thin beds of green sandstone with some limestone beds. The formation, which has thicknesses ranging from approximately 200 m to more than 1000 m near Derbendikhan (Jassim and Buday 2006a), unconformably overlies Upper Cretaceous beds, represented in the Dokan and Shaqlawa areas by Tanjero clastics and by the Maastrichtian Shiranish Formation in the Duhok area. The upper boundary is conformable and gradational with the Eocene Sinjar Formation in the Dokan area, but in the Duhok and Shaqlawa areas, the upper boundary is unconformable with the Eocene Gercus Formation (Fig. 1).

Bitumen is widespread in the outcrops of the Kolosh Formation in northern Iraq, especially in its upper part near its contact areas with the Gercus or Sinjar Formations. Bitumen occurs in two modes as main cement in bituminous sandstone: the first is a sandstone bed approximately 2–3 m thick that is fully saturated with bitumen (Fig. 2) and the second is solid bitumen filling small fissures in the sandstone, or a thin layer (less than 1 cm) wrapping sandstone balls (Fig. 3). In the Shaqlawa area, the bituminous sandstone beds are exploited to extract bitumen for industrial purposes, especially road building.

The main goals of this research are to investigate the biodegradation characteristics of bitumen and determine its source rocks.

Geological setting

The Arabian Plate is divided into the Arabian Shelf and the Arabian Shield. The Arabian Shelf, which includes Iraq, is subdivided into the Stable Shelf and Unstable Shelf. The Stable Shelf is subdivided into three zones: Rutba–Jezira, Salman and Mesopotamian, which are bounded by major faults. The Unstable Shelf is affected by the Tertiary and Cretaceous deformation and, therefore, characterised by surface folds. It comprises four zones: Imbricated, Zagros Suture, High Folded and the Low Folded (Jassim and Buday 2006b). The study area lies within the High Folded Zone (Fig. 4), which is characterised by high amplitude, long, asymmetric and faulted anticlines with northwest–southeast trends in the northeast of Iraq and east–west trends in northern Iraq. Mesozoic carbonates comprise the cores of these anticlines, whereas Tertiary carbonates and clastics lay out on their flanks. During the Palaeogene, this zone was a marginal part

of the molasse basin, while during the Late Cretaceous, it was a flysch trough (Jassim and Buday 2006a).

The basin evolution of the High Folded Zone described below is predominately based on Numan (1997), Jassim and Buday (2006b), and Aqrawi et al. (2010). Some continental blocks were separated from the northern margin of the Arabian Plate by the opening of the Neo-Tethys Ocean. During the Late Permian–Early Triassic, Iraq was located south and west of the Neo-Tethyan margin and shallow marine sediments were deposited on the passive continental margin over the Late Carboniferous unconformity. Mid-Triassic rifting led to the formation of tilted fault blocks, which were covered with a carbonate platform and fault-bounded troughs. This rifting and the formation of these blocks led to a separation of the intrashelf basins and the interior of the Arabian Plate from the Neo-Tethys. During the Triassic–Early Jurassic, extensive evaporites were deposited in the intrashelf basins in Iraq and were represented by the evaporites and carbonates of the Kurra Chine Formation, and Baluti shale, limestone and dolostones of the Mus and Butmah Formations in northern Iraq.

The intrashelf Gotnia Basin was formed at the end of the Early Jurassic and was relatively isolated from the Tethys, occupying most of Iraq. Thermal subsidence occurred on the passive continental margin and created suitable conditions for the deposition of thick sequences of carbonates in the continental slope represented by the Sarki, Sehkaniyan (Early Jurassic) and Sargelu (Middle Jurassic) Formations. To the southwest, the Butmah, Adaiya, Alan, Mus Limestone (Early Jurassic) and Muhaiwir (Middle Jurassic) Formations were deposited in neritic and lagoonal environments (Numan 1997). The organic-rich black shale and bituminous limestone of the Sargelu and Naoklekan Formations, deposited during Middle–Upper Jurassic, are considered Iraq's main Jurassic petroleum source rocks. With the opening of southern Neo-Tethys along the northern and eastern margins of the Arabian Plate during the Mid Tithonian, the deposition of evaporites in the Gotnia Basin ceased. In the Late Tithonian the subduction of the oceanic crust of the Arabian Plate under the Turkish and Iranian Plates commenced and the Gotnia Basin was succeeded by the Balambo–Garau Basin in which the organic-rich shale and limestone of the Chia Gara Formation was deposited; this formation is considered important for source rocks for hydrocarbons (Fig. 1). In addition, approximately 500 m of basinal sediments were deposited during the Turonian–Early Campanian in that basin. Ophiolites were obducted on the Arabian Plate in the Late Campanian–Early Maastrichtian leading to the formation of a narrow foreland basin around the eastern and northern margin of the Arabian Plate. The ophiolites and associated sedimentary rocks, which uplifted above the sea level, were eroded and re-deposited as thick (about 2 km) flysch deposits in the foredeep basin. The southern Neo-Tethys was completely closed in the Early

Fig. 1 Stratigraphic column of North Iraq and the position of the proposed source rocks and the bitumen samples
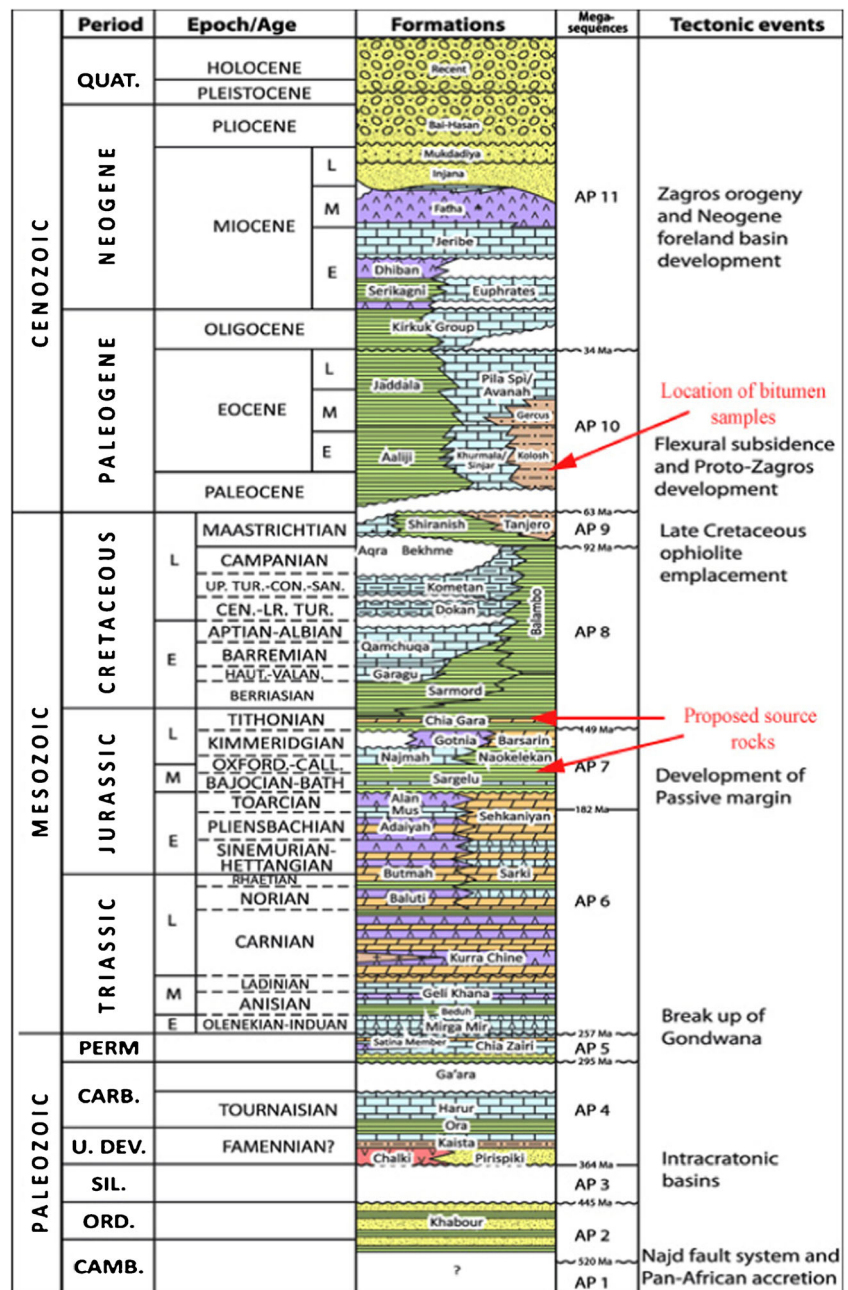
Maastrichtian. A new depocenter (called the Palaeogene Mesopotamian Basin) was formed after the uplifting of the northeast area of the former Late Cretaceous foreland basin. The erosion of the flanking thrust belt during uplift in the Palaeocene led to deposition of Kolosh and Gercus clastic sediments, which prograded from the Zagros to the basin's centre. The Kolosh Formation was deposited in a relatively narrow foredeep basin, which was developed during the Early Palaeocene and progressively migrated to the southwest. In Iraq, Oligocene successions are restricted to a small area (the axial part of the foreland basin) and are absent in other areas. Carbonate, evaporite and clastic sediments of the Fat'ha and

Injana Formations filled the foreland basin during Middle–Upper Miocene. The molasse sediments of the Pliocene Mukdadiya and Bai Hassan Formations were deposited over the Upper Miocene Injana Formation in most areas of northern Iraq.

Materials and methods

Nine samples from the Kolosh Formation were taken from three sites (Duhok, Shaqlawa and Dokan; Fig. 4, Table 1). Seven samples (Nos. 1, 2 and 5–9) are bituminous sandstone

Fig. 2 Sandstone saturated with migrated bitumen in the upper part of the Kolosh Formation close to its upper contact with the Gercus Formation in the Bekher anticline, Duhok area (hammer length is 35 cm)

while the other two (Nos. 3 and 4) are solid bitumens from Shaqlawa and Dokan and were picked from fractures and from sandstone balls (Fig. 3).

For saturated and aromatic biomarkers and other geochemical analyses, extractable organic matter (EOM) was taken from the nine samples using dichloromethane as the solvent in a Dionex ASE 200 accelerated solvent extractor. An excess of hexane was added to precipitate the asphaltenes. The deasphalted extract was then split into three fractions: saturates, aromatics and NSO compounds using column chromatography on silica gel. The solvents used were pentane, pentane–dichloromethane (40/60 v/v) and methanol, respectively. The percentage of each fraction was determined after the evaporation of the solvent.

Gas chromatography of the saturated hydrocarbon fraction was performed using a Hewlett Packard Series II 5890 GC. The program of the oven temperature was 20 °C for 5 min to 310 °C for 20 min at a rate of 4 °C/min. Analysis of the saturated and aromatic hydrocarbon biomarkers was carried out using a Finnigan TSQ-70 mass spectrometer coupled to a

Fig. 3 Sandstone ball covered with a thin crust of solid bitumen in the Shaqlawa area (pen length is 14 cm)

Hewlett Packard Series II 5890 gas chromatograph in full scan mode. The temperature conditions of the GC-MS were programmed from 40 °C for 2 min to 310 °C for 30 min at a rate of 4 °C/min.

Isoprime vario ISOTOPE select elemental analyser and VisION isotope ratio mass spectrometer (IRMS) were used for analysis of the stable carbon isotope compositions of aromatics, NSO and asphaltene fractions. Carbon isotope ratios of saturates were not determined due to their extremely low concentrations. Results are reported relative to Vienna Pee Dee Belemnite (‰/VPDB). The stable hydrogen isotope (deuterium) was determined for resins and asphaltenes, which form the main components of the bitumens (more than 90%). Isotopic compositions of the deuterium are given in the delta notation relative to Vienna Standard Mean Ocean Water (‰/VSMOW).

Results

Bulk composition

The EOM yields of samples analysed are consistent with their mode of occurrence, mainly as a sandstone cement, and range from 4485 to 84,140 ppm by weight (Table 1). The highest value was recorded from the solid bitumen sample from the site at Shaqlawa (84,140 ppm in sample No. 4). All samples exhibited a high content of sulphur (7.4–10.6%) and polars (NSO + asphaltene) (90.0–96.4%), and a low amount of saturates (0.7–8.9%) and aromatics (1.9–8.6%) in the EOM (Table 1, Fig. 5). The saturates/aromatics ratio is generally less than one, except in sample 1, which has a value equal to 1. There was one notable exception: the solid bitumen sample No. 4 from the Shaqlawa area had higher saturates and aromatics and a lower percentage of polar fractions (8.9%, 24.2% and 66.8% respectively; Table 1).

Gas chromatography (GC)

The GC chromatogram of most samples showed unresolved complex mixtures (UCM) with a few peaks represented by C_{29}–C_{35} hopanes and gammacerane, which appear at the tail of the chromatograms (Fig. 6). In the Duhok samples and some of those from Shaqlawa, the normal alkanes and isoprenoids are either totally removed or are present in very low concentrations (sample 7; Fig. 6) due to surface contamination by recent organic matter, as indicated by the presence of normal alkanes with an even predominance of C_{16}, C_{18} and C_{20}, which was unexpected in these asphalts. The Pr/Ph ratio of the three samples is relatively high (more than 1) and supports the contamination explanation. It is well established that normal alkanes and isoprenoids are initially removed during biodegradation (Connan 1984; Peters et al. 2005). In these

Fig. 4 Map of Iraq showing the main tectonic zones and the study areas
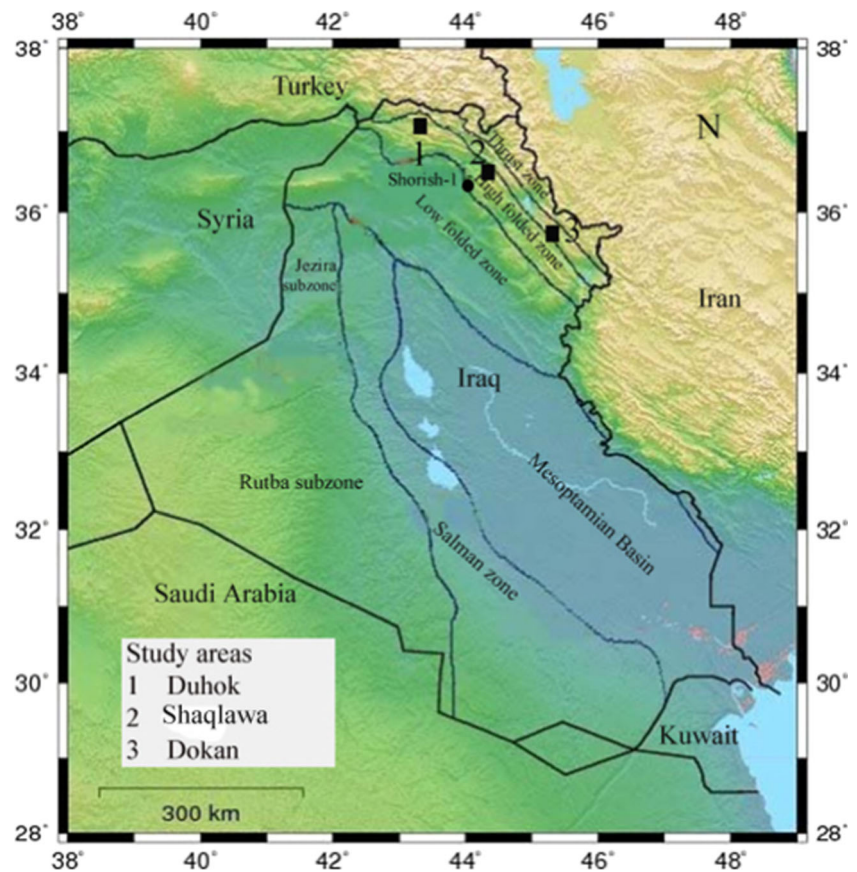
samples, normal alkanes, in the range of C12–C22, and isoprenoids (pristane and phytane) are present when hopanes and steranes are biodegraded, and are, therefore, exogenous and products of contamination. In addition, some samples (6 and 7) contain normal alkanes, but their terpanes are biodegraded (hopanes and/or steranes); therefore, these normal alkanes are contaminant; but the biomarker ratios are not affected by this contamination. For instance, the Gammacerane/C31$\alpha\beta$Hopane ratio of these samples is inscribed in the general trend as seen in Fig. 9.

Gas chromatography–mass spectrometry (GC–MS)

The m/z 191 mass chromatograms of the samples analysed are characterised by the dominance of C_{30} hopane, C_{29} norhopane, Ts, Tm and gammacerane (Fig. 7), with minor concentrations of C_{20}–C_{31} tricyclic terpanes. Extended hopanes are fully developed in most samples and hexahydrobenzohopanes ($C_{32/6}$–$C_{35/6}$; Connan and Dessort 1987) are significantly enriched in some samples, which indicate significant biodegradation in terpanes.

C_{30} hopane and regular sterane concentrations are highly variable among the studied samples, ranging between 24–657 and 20–388 ppm, respectively. In addition, Ts/Ts + Tm is generally less than 0.24 but with one sample having a higher value

(0.70; Table 2). The moretane/hopane, gammacerane/C_{30} hopane ratio is highly variable being between 0.07–5.37 and 0.14–5.70, respectively (Table 2). The 22S/22S + 22R ratio of the C_{31}–C_{35} hopanes are highly variable with the ratio reaching the equilibrium for some samples while others are lower and higher than the equilibrium values (Table 4).

Regular sterane distribution shows the dominance of C_{29} over C_{28} and C_{27} steranes in all samples. C_{29} S/S + R and $C_{29}\beta\beta$S/$\beta\beta$S + $\alpha\alpha$R sterane ratios are generally below the equilibrium values (Table 3). The diasteranes/regular sterane ratio is generally low, except for the two solid bitumen samples where they have higher values (Table 3).

Carbon and hydrogen isotopes

Carbon isotopes of the aromatic, resin (NSO) and asphaltenes of all samples are very close: between − 28.0 and − 27.1, − 27.9 and − 27.6, and − 28.1 and − 27.7‰/VPDB for aromatic, resin and asphaltenes, respectively (Table 1). Their carbon isotope ratios were not determined due to the low concentration of saturates. Deuterium isotope ratios were also measured for resin and asphaltenes in high-percentage extracts to monitor the oxidation effect on bitumens. Deuterium isotope values have a wider range than carbon isotope ratios: between

Table 1 Bulk geochemical, stable isotopes and sulphur data of the bitumen samples

Number	Location	Type	Group	Sat.%	Arom.%	NSO.%	Asph.%	Sat/Aro	EOM (ppm)	Sulphur %	$\delta^{13}C$ Aro (‰/VPDB)	$\delta^{13}C$ Res (‰/VPDB)	$\delta^{13}C$ Asph (‰/VPDB)	δD Res (‰/VSMOW)	δD Asph (‰/VSMOW)
1	Shaqlawa	Bitum. Sst	1	1.9	1.9	15.6	80.5	1.0	19,157	10.3	–	−27.8	−27.9	−78.9	−67.9
2	Shaqlawa	Bitum. Sst	2	1.2	3.2	15.8	79.8	0.38	20,959	10.7	−27.8	−27.9	−28.1	−75.6	−70.5
3	Dokan	Solid Bit.	2	3.7	5.4	24.8	66.1	0.68	18,744	6.6	−27.1	−27.8	−27.9	−81.1	−76.6
4	Shaqlawa	Solid Bit.	1	8.9	24.2	16.3	50.5	0.37	84,140	7.4	−27.6	−27.7	−27.9	−98.0	−95.7
5	Duhok	Bitum. Sst	1	1.5	8.5	15.0	75.0	0.17	27,397	8.7	−27.6	−27.6	−28.0	−77.2	−79.2
6	Shaqlawa	Bitum. Sst	2	1.1	4.2	16.3	78.4	0.26	21,701	9.0	−27.3	−27.8	−27.9	−75.7	−74.5
7	Duhok	Bitum. Sst	2	1.4	2.2	17.7	78.7	0.67	4485	9.7	–	−27.8	−27.7	−79.0	−65.7
8	Duhok	Bitum. Sst	2	1.4	4.3	15.0	79.3	0.32	33,185	9.2	−28.0	−27.6	−27.9	−69.5	−71.4
9	Duhok	Bitum. Sst	1	0.7	7.3	19.6	72.4	0.09	29,672	9.7	−27.6	−27.8	−28.0	−69.9	−93.9

EOM, extracted organic matter; δD, deuterium isotope

Fig. 5 Ternary diagram showing the composition of the bitumen being studied (see Table 1 for sample information). Note that sample 4 is the least biodegraded
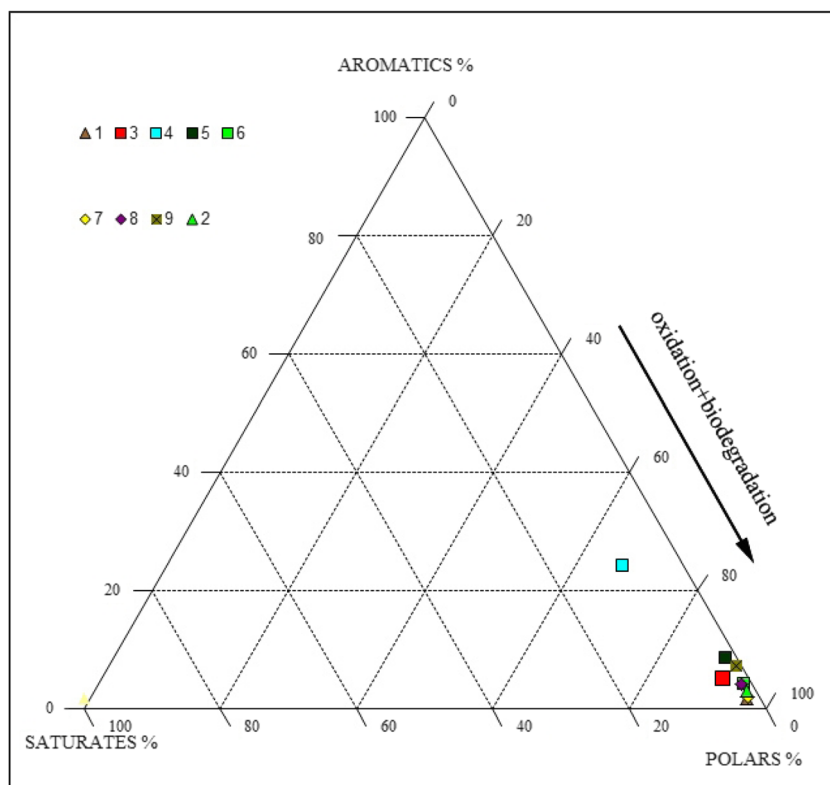
−98.0 and −69.5‰ for resin and −95.7 and −65.7‰ for asphaltenes (Table 1).

Discussion

Biodegradation

The very high percentage of sulphur (more than 6.6%/weight) and the low percentage of saturates and aromatics in most samples associated with the high percentage of resins and asphaltenes (Table 1) suggest that the samples are biodegraded (Fig. 5) as they are located in a well-documented area of archaeological bitumens and oil seeps, and gas chromatograms of these samples support this (Fig. 6). All normal alkanes and isoprenoids of the original bitumen are totally removed, suggesting a degree of biodegradation that is higher than five (Peters and Moldowan 1993).

Gammacerane, moretane, Ts, Tm, 18α(H)–oleanane and C_{29} hopane remain fairly stable during biodegradation (Seifert et al. 1984; Lin et al. 1989) and are valid compounds for correlation purposes. According to the relative abundance of these biomarkers, the samples can be divided into two groups based on their degrees of biodegradation: Group 1 includes four samples (Nos. 1, 4, 5 and 9) while Group 2 includes the other samples (Nos. 2, 3 and 6–8).

Group 1 is characterised by a total lack of normal alkanes and isoprenoids with preserved or slightly degraded terpanes

and steranes. These samples are moderately biodegraded and represent levels 5–6 on the Peters and Moldowan scale (1993). They have relatively high concentration of C_{30} hopane (234–657 ppm), moderate values of C_{29}/C_{30} hopane, low-ratio values of moretane/hopane, $C_{31}R/C_{30}$ hopane, gammacerane/$C_{31}R$ hopane, diahopane/C_{30} hopane and tricyclic terpanes/C_{30} hopane (Tables 2 and 3). In addition, these samples contain the full series of C_{31}–C_{35} hopanes (Fig. 7).

Group 2 samples are characterised by the total removal of normal alkanes and isoprenoids, with hopanes and steranes degraded to different extents. These samples have a relatively high concentration of resistant molecules to biodegradation, such as C_{29} hopane, moretane, gammacerane, Ts and hexahydrobenzohopanes. Therefore, they exhibit high values for all the ratios mentioned previously; their demethylated hopane/C_{30} hopane ratio ranges between 0.02 and 0.10 (Table 2), suggesting that these bitumens are heavily biodegraded (Peters et al. 2005). None of these samples show a full series of demethylated hopanes.

The very low concentration of 25-norhopanes in these samples may be due to a state of biodegradation that had not reached the limit required for their formation, an assumption supported by the presence of well-developed extended hopanes in most samples. However, the depositional environment, which will be discussed later, indicated that these bitumens were generated from carbonate source rocks and the biodegradation of hopanes in these would not have led to the formation of 25-norhopanes (Blanc and Connan 1992).

Fig. 6 Gas chromatograms of saturate fraction for all samples showing the removal of normal alkanes and isoprenoids of some samples (see Table 1 for sample information)
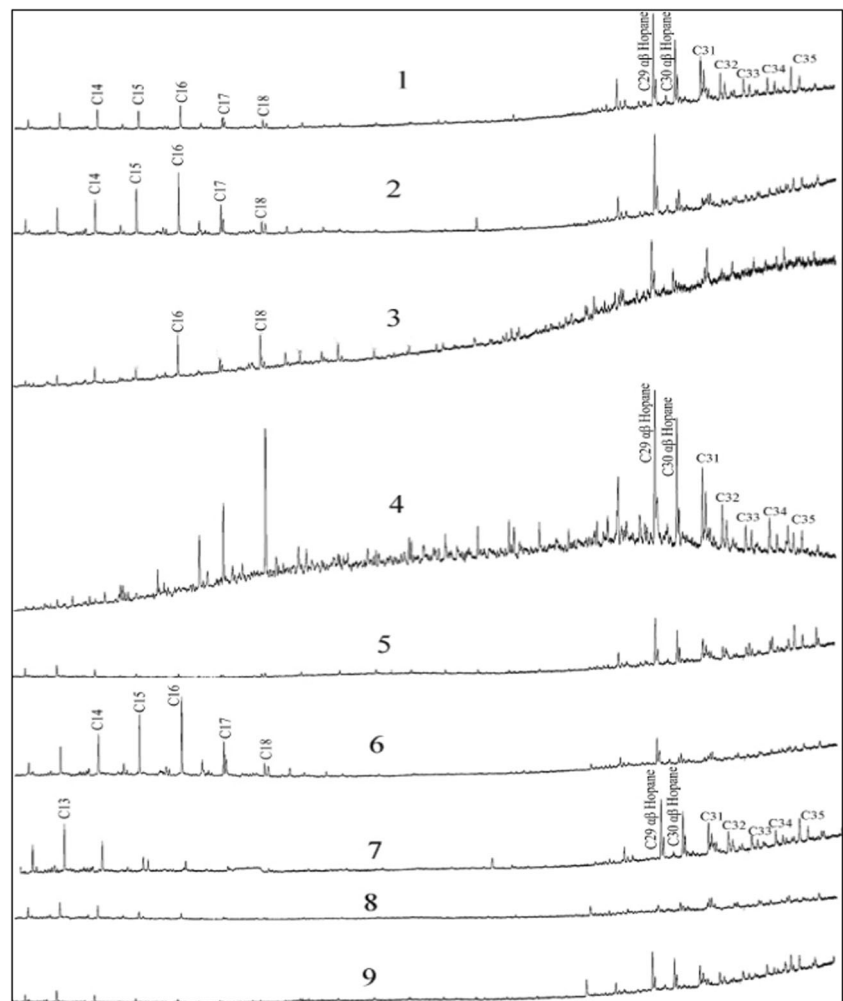
The samples analysed were taken from the surface of outcrops exposed to atmospheric conditions millions of years ago. The degradation of hopanes under aerobic conditions takes place without the formation of 25-norhopanes, as documented from seep oils around the world (Moldowan et al. 1992; Wenger and Isaksen 2002; Bennett et al. 2006) and from Grosmont Formation bitumen in Alberta, Canada (Bennett and Larter 2018; Park et al. 2018). This assumption is supported by laboratory experiments (Bost et al. 2001; Frontera-Suau et al. 2002; Watson et al. 2002).

Moretane is less thermally stable than hopane so the moretane/hopane ratio will decrease with increasing maturity (Peters et al. 2005). It is also known that hopanes biodegrade more rapidly than moretanes (Connan 1984); therefore, the moretane/C_{30} hopane ratio will increase with biodegradation. The moretane/hopane ratio of Group 1 is less than 0.10, while it is more than 0.21 in Group 2 (the value for No. 8 is very high at 5.37; Table 2). The abundance of C_{30}–C_{35} $\alpha\beta$-hopanes relative to more resistant compounds, such as gammacerane, is controlled by the degree of biodegradation (Seifert and Moldowan 1979; Seifert et al. 1984); therefore, the

gammacerane/C_{31}R hopane and gammacerane/C_{30} hopane ratios can be used to monitor the effect of degradation as gammacerane is a more resistant biomarker and less biodegraded. These ratios are low (less than 0.81 and 0.32, respectively) in the less degraded samples (Group 1) and high to very high (more than 2 and 1, respectively) in the moderately to heavily degraded samples of Group 2 (Table 2; Figs. 8 and 9). The Gammacerane/C30 hopane ratio of the oil produced from the Shorish well in Kurdistan region is 0.17 (Sachsenhoger et al. 2015). This value is close to the less biodegraded sample of the present study (sample 4). This characteristic indicates that biodegradation is the main cause which affects the hopane concentration in the bitumen samples. When the absolute amount of hopane decreases in the alkane fraction, the gammacerane to $C31\alpha\beta$ Hopane increases.

The 18α-22, 29, 30-trisnorneohopane (Ts)/17α-22, 29, 30-trisnorhopane (Tm) ratio is widely used as maturity parameter up to level 9 of the biodegradation scale after Peters and Moldowan (1993), although it is affected by lithology (Peters et al. 2005) and biodegradation (Bost et al. 2001;
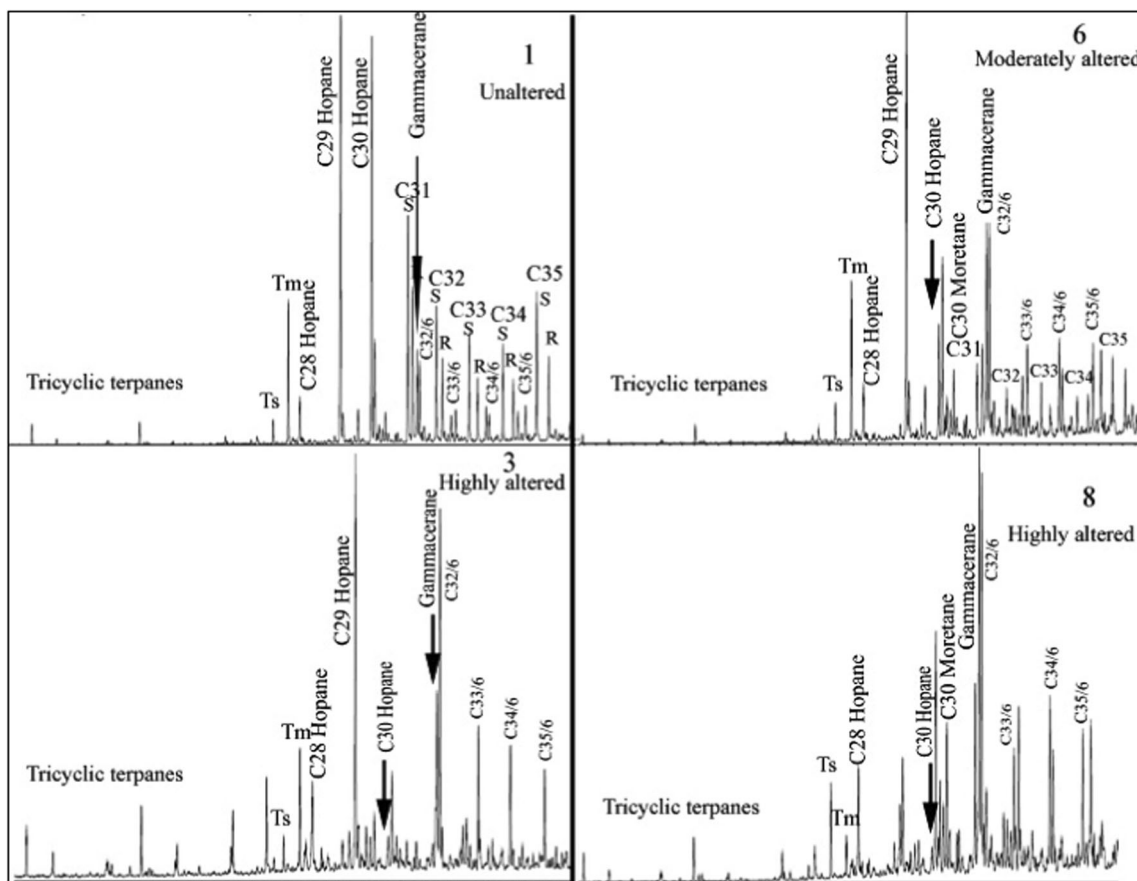
Fig. 7 Mass chromatograms of the terpanes ($m/z = 191$) of selected bitumen samples (see Table 1 for sample information) with different biodegradation levels

Bennett and Larter 2018). The latter authors observed that the high Ts/Ts + Tm ratio of the biodegraded bitumens of the Grosmont Formation in Canada was associated with the lowest concentration of Tm because Tm is more susceptible to biodegradation than Ts (Bost et al. 2001; da Cruz et al. 2008; Bennett and Larter 2018). Sample 8 shows high values for the ratios Ts/Ts + Tm (0.70, Table 2), C_{29} 20S/20S + 20R (0.60), C_{29} $\beta\beta/\alpha\alpha + \beta\beta$ (0.67, Table 3), diahopane/C_{30} hopane and

Table 2 Biomarker ratios of the hopanes and some aromatic biomarkers

Sample	$C_{29}/$ H	$C_{30}X/$ H	M/ H	$C_{31}R/$ H	GA/ $C_{31}R$	GA/C_{30} hopane	C_{35}/C_{30} hopane	$C_{35}S/$ $C_{34}S$	Homo. index	Ts/ Ts + Tm	DM/ H	T/H	DBT/ P	MDBT/ MP	CR	DR	MDR
1	1.05	0	0.07	0.38	0.58	0.22	0.57	1.53	0.20	0.15	0	0.23	0.07	0.23	0.07	0.80	2.88
2	4.26	0.02	0.36	0.52	2.04	1.06	1.19	1.93	0.28	0.13	0.02	0.51	0.08	0.30	0.02	0.82	3.50
3	13.43	0.20	0.21	0.75	7.63	5.70	0.60	0.85	0.11	0.22	0.10	11.23	0.09	0.42	0.04	0.89	1.86
4	1.07	0.01	0.09	0.39	0.35	0.14	0.29	0.99	0.11	0.24	0.01	0.50	0.11	0.97	0.01	0.77	3.25
5	1.21	0.01	0.10	0.38	0.81	0.31	0.70	1.53	0.22	0.15	0	0.20	0.14	0.29	0.01	0.79	2.84
6	3.75	0.03	0.58	0.53	3.42	1.81	1.12	1.77	0.26	0.20	0.03	0.76	0.08	0.34	0.01	0.81	3.87
7	1.03	0	0.07	0.34	0.70	0.24	0.64	1.43	0.21	0.13	0	0.05	0.07	0.23	0.04	0.84	2.74
8	2.50	0.30	5.37	0.47	3.37	1.57	2.10	3.13	0.24	0.70	0.04	8.17	0.27	0.56	0.01	0.83	2.26
9	1.02	0	0.07	0.35	0.66	0.23	0.64	1.54	0.22	0.13	0	0.12	0.19	0.53	0.02	0.83	2.97

C_{29}/H, C_{29}/C_{30} hopane; $C_{30}X/H$, diahopane/C30 hopane; M/H, moretane/hopane; GA/$C_{31}R$, gammacerane/C_{31} R hopane; Homo. index, homohopane index = ($C_{35}/C_{31}–C_{35}$); DM/H, demethylated hopane/C_{30} hopane; T/H, tricyclic terpanes/C_{30} hopane; DBT/P, dibenzothiophene/phenanthrene; MDBT/MP, methyldibenzothiophene/methylphenanthrene = sum of MDBT/MP; CR, cracking ratio of the triaromatic steranes = ($C_{20} + C_{21}$)/($C_{20} – C_{28}$) triaromatic sterane; DR, triaromatic dinosteroid ratio = [(D1 − D6)/((D1 − D6) + 4-methylstigmastanes (20S + 20R)]; MDR, methyldibenzothiophene ratio = 4-MDBT/1-MDBT

Fig. 8 Cross-plot of the carbon isotope of the asphaltene fraction versus gammacerane/C_{30} hopane of the bitumen samples (see Table 1 for sample information). The plot separates between the more biodegraded samples (Group 2; samples 2, 3, 6, 7, 8) and the less biodegraded samples (Group 1; samples 1, 4, 5, 9)
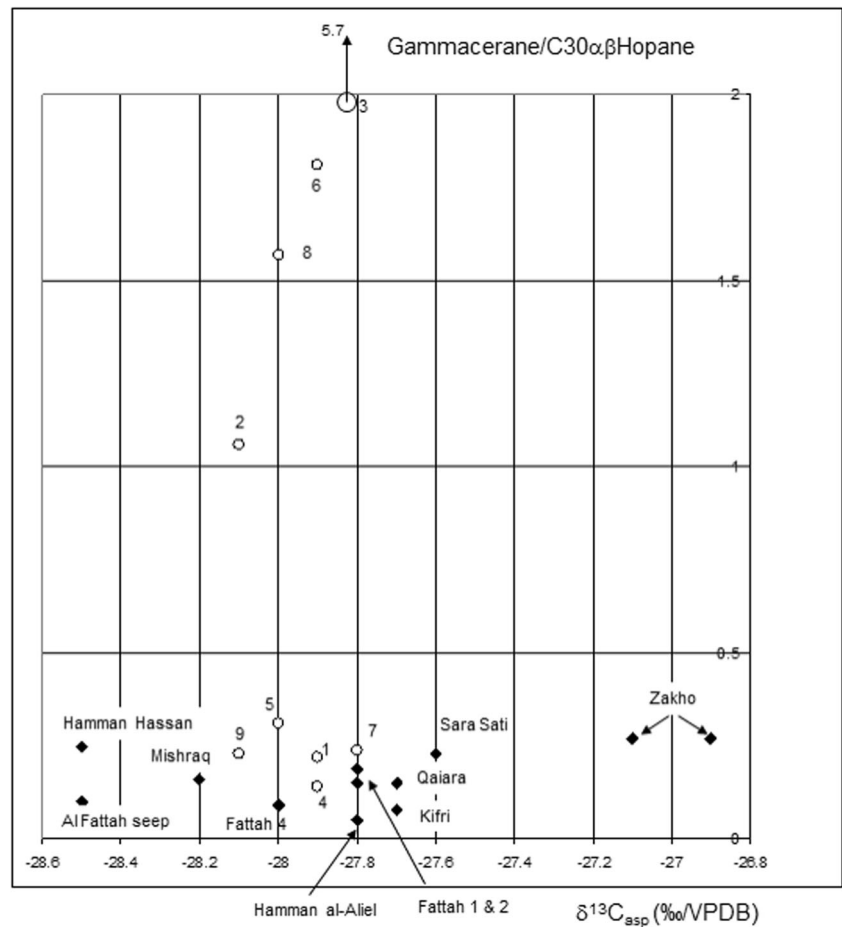
moretane/hopane. These high values are associated with the lowest concentration of C_{30} hopane, Tm and C_{27} steranes in all samples. The lowest concentration of C_{27} steranes in

sample No. 8 could be attributed to biodegradation; C_{27} steranes are less resistant to biodegradation than C_{29} steranes (Goodwin et al. 1983; Volkman et al. 1983; Connan 1984;

Fig. 9 Cross-plot of the C_{30} hopane concentration versus the gammacerane/C31 R hopane of the bitumen samples (see Table 1 for sample information). The plot separates between the more biodegraded samples (group 2) and the less biodegraded samples (group 1)
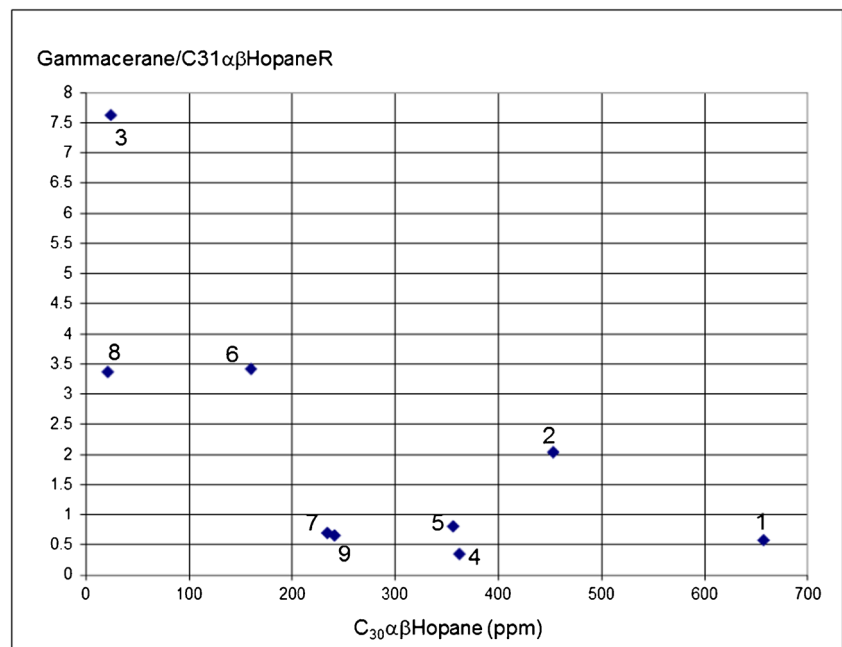
Table 3 Sterane biomarker ratios

Sample	Location	Type	Group	Ster/ Hop.	Dia/ Reg	C27%	C28%	C29%	C29S/ S + R	C29ββS/ ββS + ααR
1	Shaqlawa	Bitum. Sst	1	0.07	0.10	19.9	23.0	57.1	0.44	0.43
2	Shaqlawa	Bitum. Sst	2	0.08	0.12	11.5	21.2	67.3	0.39	0.33
3	Dokan	Solid. Bit.	2	0.07	0.43	23.0	25.9	51.1	0.30	0.24
4	Shaqlawa	Solid Bit.	1	0.18	0.21	32.7	23.5	43.8	0.35	0.47
5	Duhok	Bitum. Sst	1	0.09	0.11	13.7	22.7	63.6	0.40	0.52
6	Shaqlawa	Bitum. Sst	2	0.09	0.07	14.1	23.1	62.8	0.35	0.35
7	Duhok	Bitum. Sst	2	0.02	0.16	5.8	21.3	72.9	0.19	0.16
8	Duhok	Bitum. Sst	2	0.11	0.14	4.6	19.9	75.5	0.60	0.67
9	Duhok	Bitum. Sst	1	0.03	0.09	17.2	23.1	59.7	0.29	0.31

Peters et al. 2005). Moreover, in non-biodegraded samples there are no 20S/20S + 20R values above the endpoint (0.56) and higher values of this ratio indicate selective biodegradation of steranes (Peters et al. 2005). The high and anomalous C_{29} 20S/20S + 20R and C_{29} ββ/αα + ββ values (0.60 and 0.67, respectively) of sample No. 8 are due to partial degradation of the biological configuration αα20R steranes (Peters and Moldowan 1993; Fig. 10). The preferential removal of this isomer is also documented through laboratory experiments where the aerobic bacterial culture degraded the hopanes without the formation of 25-norhopanes (Chosson et al. 1992). These facts clearly indicate that the hopanes and

steranes of this sample are heavily biodegraded and that C_{27} steranes are highly biodegraded relative to C_{29} steranes (Fig. 10). In addition, sample No. 7 has low C_{29} 20S/20S + 20R and C_{29} ββ/αα + ββ ratios (0.19 and 0.16, respectively) in comparison to other samples (Table 3), but its terpane maturity parameters are similar. These low values are associated with low saturated and aromatic content, low percentage C_{27} steranes and high diasterane/regular steranes relative to other samples (Table 3). These variations can be attributed to the partial degradation of steranes, whereas hopanes show an unaffected pattern. These observations indicate that steranes were degraded prior to hopanes, as found by Seifert et al.

Fig. 10 Mass chromatogram of the steranes ($m/z = 217$) of selected bitumen samples (see Table 1 for sample information) with different biodegradation level
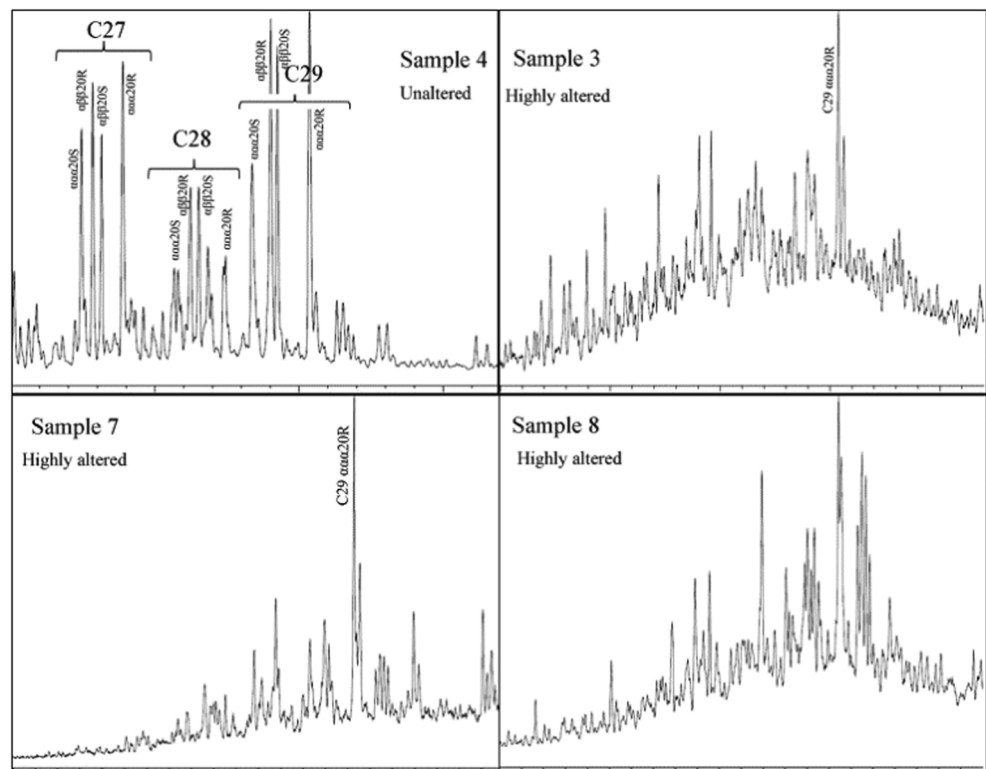
(1984) in seep oils in Greece. The features previously mentioned suggest that Group 1 samples are moderately biodegraded (levels 5–6 of Peters and Moldowan 1993) while Group 2 samples are heavily to very heavily biodegraded (levels 7–8). Biodegradation enhanced the concentration of C_{32}–C_{35} hexahydrobenzohopanes in the moderately to heavily biodegraded samples (Fig. 7) by removal of extended hopanes. These compounds were recorded in the biodegraded bitumens of Grosmot Formation (Bennett and Larter 2018).

The 22S/22S + 22R ratios (Table 4) for Group 1 samples and No. 7 of Group 2 samples reached equilibrium values (0.59–0.64) although a slight variation of this ratio was observed indicating that C_{31}–C_{35} hopanes are not affected by biodegradation or that the two isomers (S and R) are affected to the same extent.

By contrast, Group 2 samples show high variations in this ratio among the C_{31}–C_{35} hopanes but without a systematic trend from C_{31}–C_{35}. The samples may be split into two subgroups. Those in Group 2A are moderately biodegraded (Nos. 2 and 6) and show a slight predominance of 22R over 22S for the C_{34} hopane and a reversed situation in other homologues (Table 4, Fig. 11). Group 2B includes two samples (Nos. 3 and 8) with No. 3 showing a preferential degradation of 22S relative to 22R for C_{31}–C_{32} hopanes and, to a lesser extent, for C_{34} hopane, which led to a decrease in the 22S/22S + 22R ratio. Other homologues (C_{33} and C_{35}) are slightly affected or not affected at all. In sample No. 8, 22S is preferentially degraded relative to 22R for C_{32} and C_{34} hopanes, entailing a strong predominance of 22R over 22S. A reverse situation is recorded for C_{33} hopanes; C_{31} is slightly affected whereas C_{35} is unaffected by biodegradation when compared to less degraded samples (Fig. 11). The degradation behaviour of samples from the present study contrasts with the most published research (e.g. Goodwin et al. 1983; Connan 1984; Bennett and Larter 2018), which reported that the 22R isomer of extended hopanes are more affected by biodegradation than that of 22S. However, the degradation pattern of the samples from the present study is similar to the biodegradation of the C_{31}–C_{35} hopanes of the oils of western Siberia and San Joaquin, and is consistent with the calculations of molecular mechanics that support the preferential degradation of 22S of the C_{31}–C_{33} hopane of those oils (Peters et al. 1996). The slight preservation of C_{35} hopane in all samples relative to other homologues concurs with previous studies (Requejo and Halpern 1989; Moldowan et al. 1995; Bost et al. 2001). C_{35} hopanes are more resistant to biodegradation than other C_{31}–C_{34} hopanes (Bennett and Larter 2018) and the C_{35}/C_{30} hopane ratio is low to medium (0.29–0.70) in the less altered samples and medium to high in the most degraded samples (0.60–2.10). The highest value of this ratio was recorded in sample No. 8, which has the lowest concentration of C_{30} hopane (21 ppm of C_{30} hopane), indicating more degradation of the C_{30} hopane relative to the C_{35} hopane (Bost et al. 2001) and supporting the conservative behaviour of C_{35} during biodegradation.

Abiotic oxidation effect

The δ^{13}C of asphaltene is used as a tool for correlation between severely degraded bitumens (Connan 1999). The δ^{13}C values of the asphaltene and resin fractions of the samples show almost identical values (a deviation of less than 0.5‰/ VPDB; Fig. 12), which indicate that these bitumens have a common origin.

The δD values of polar fractions are strongly affected by alteration processes and are, therefore, not useful in establishing the correlation between samples. The δD values of asphaltene and resin fractions of bitumen samples show that some samples have oxidised to different degrees. The δD values of asphaltenes (in ‰/VSMOW) increase from − 95.7‰ in samples that have the lowest level of oxidation and biodegradation (Nos. 4 and 9) to − 65.7‰ in those that are most oxidised and biodegraded (Table 1). The δD of sample Nos. 4 and 9 shows values very close to those observed in crude oils from oilfields in Iraq and Iran (Stern et al. 2008;

Table 4   22S/22S + 22R ratio of the C_{31}–C_{35} hopanes of the bitumen samples

Sample	Location	Type	Group	31S/ S + R	32S/ S + R	33S/ S + R	34S/ S + R	35S/ S + R
1	Shaqlawa	Bitum. Sst	1	0.60	0.62	0.63	0.61	0.64
2	Shaqlawa	Bitum. Sst	2	0.55	0.65	0.66	0.49	0.53
3	Dokan	Solid Bit.	2	0.34	0.16	0.68	0.48	0.54
4	Shaqlawa	Solid Bit.	1	0.59	0.60	0.61	0.59	0.62
5	Duhok	Bitum. Sst	1	0.60	0.63	0.64	0.62	0.62
6	Shaqlawa	Bitum. Sst	2	0.55	0.64	0.69	0.49	0.52
7	Duhok	Bitum. Sst	2	0.62	0.65	0.66	0.64	0.63
8	Duhok	Bitum. Sst	2	0.57	0.13	0.74	0.33	0.66
9	Duhok	Bitum. Sst	1	0.61	0.64	0.64	0.61	0.61

Fig. 11 Variation of the 22S/ 22S + 22R ratio of the homohopanes of selected bitumen samples (see Table 1 for sample information). The more biodegraded samples (3 and 8) have low 22S/22S + 22R ratio of C32 and C34
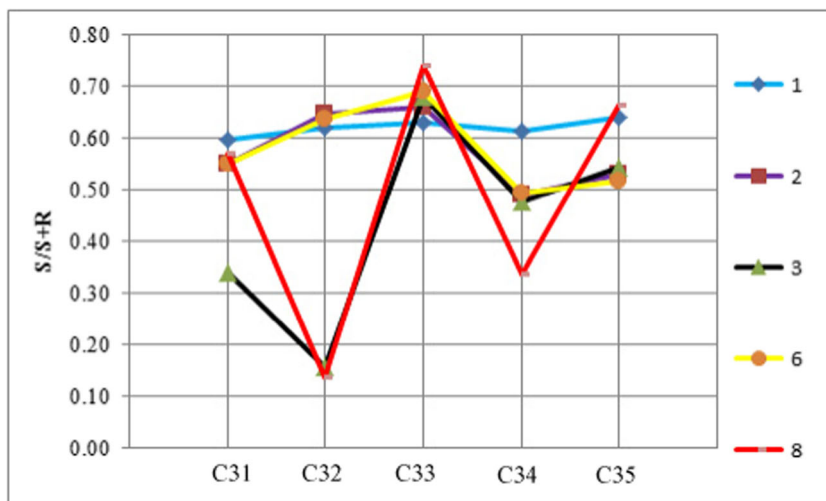

Fig. 12), indicating that they are unoxidised to slightly oxidised, whereas other samples are obviously oxidised. They display δD values matching those observed in archaeological samples from Sri Lanka (Stern et al. 2008; Fig. 12). Sample No. 7, which has the highest enrichment of deuterium in asphaltene (i.e. highest level of oxidation), also has an advanced level of biodegradation as seen previously. δD of resins (Fig. 13) confirm that this polar fraction is also affected by oxidation. Sample No. 4 seems to have well-preserved asphaltene and resins whereas sample No. 9 appears to have affected resins with preserved asphaltene. This assumption is reasonable for oxidation begins with aromatics then continues

with resins and finally ends with asphaltene. The increased deuterium content in the asphaltene of the present study is very similar to that of the Hit bitumens published by Charrié-Duhaut et al. (2000) in which they observed increasing δD values with increasing alteration from − 92‰/ VSMOW in the less altered sample to − 68‰/VSMOW in the most altered ones. The increased deuterium content in asphaltene is attributed to exchange reactions with percolating rainwater (Charrié-Duhaut et al. 2000). In addition, Asif et al. (2009) showed that normal alkanes with low molecular weights (C_{14}–C_{22}) of lightly biodegraded oils had the largest deuterium enrichment: up to 50% with biodegradation, while

Fig. 12 Cross-plot of the carbon isotope of the asphaltene fraction versus the hydrogen isotope (deuterium) of the bitumen samples (see Table 1 for sample information). The least oxidized and biodegraded samples (4 and 9) are well separated
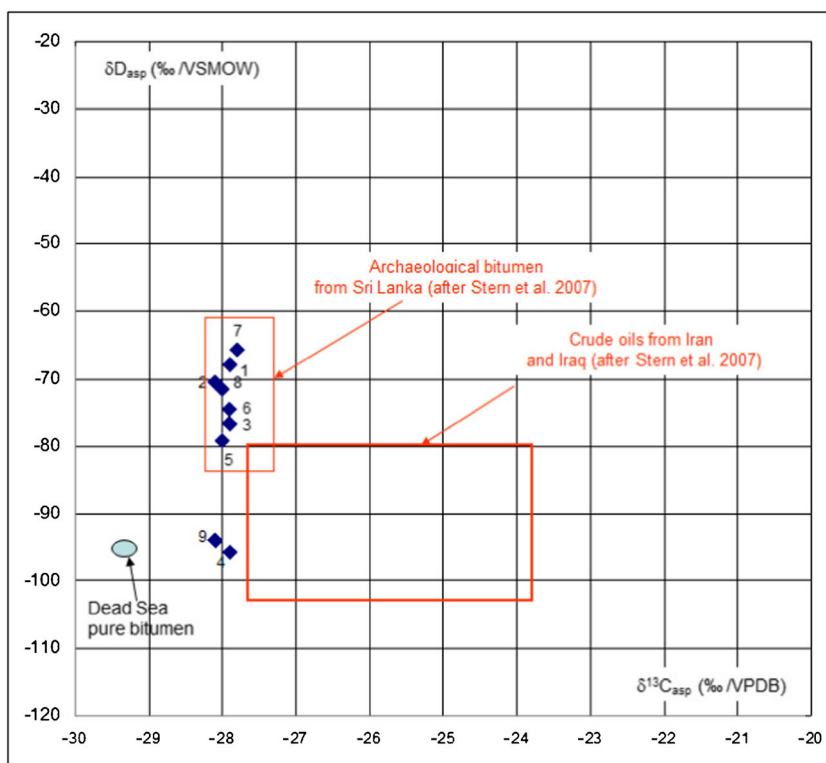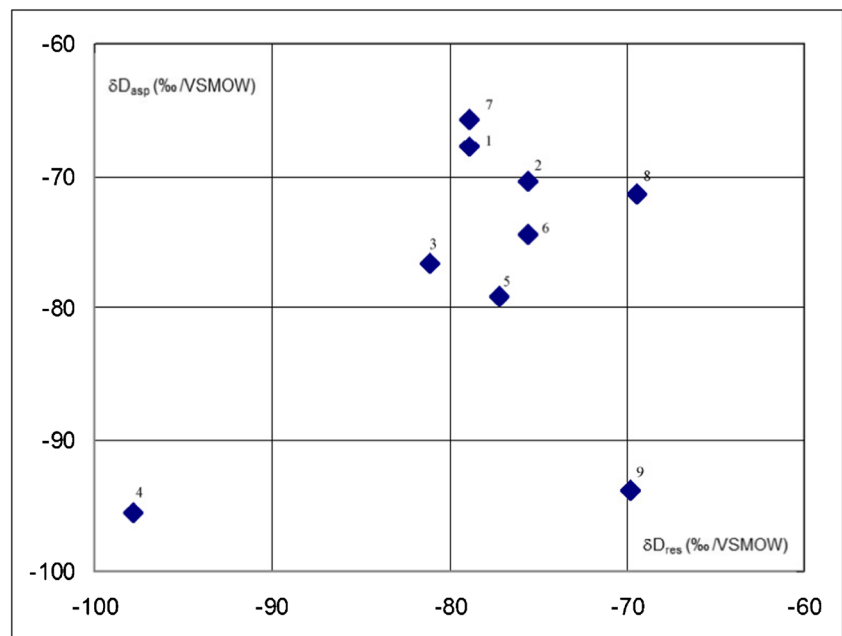
Fig. 13 Cross-plot of the
hydrogen isotopes (deuterium) of
the asphaltene versus resin of the
bitumen samples (see Table 1 for
sample information). The least
oxidized and biodegraded
samples (4 and 9) are well
separated

normal alkanes with high molecular weights ($> C_{23}$) had a
smaller enrichment. However, Sun et al. (2005) observed a
small increase in the deuterium content of normal alkanes
from − 175‰/VSMOW in the non-biodegraded oils to −
145‰/VSMOW in those that were heavily biodegraded,
which suggested small fractionation.

Polar compounds of oil seepages do not show systematic
changes with biodegradation levels, and source-rock charac-
teristics and maturity may influence polar content (Hosseini
et al. 2018). By increasing the intensity of biodegradation, the
sulphur and asphaltene content will increase, and saturated
and aromatic hydrocarbon content will decrease leading to a
decrease in the API gravity of residual oil (Larter et al. 2006;
Lopez et al. 2015). Moreover, during biodegradation (or at
least in the first stages), saturated hydrocarbons are easily
removable, while sulphur in organic matter and organic com-
pounds is not easily released, leading to an increase in the
sulphur content in biodegraded oils (Orr 1978). The
saturated/aromatic hydrocarbon ratio in all samples is equal
to or less than 1, and the aromatic percentage rises from very
low (3.6%) in most altered samples to 24.2 in less altered ones.
The percentage of saturated hydrocarbons is also low in the
highly degraded samples, but generally higher than those of
aromatics indicating they are also subjected to abiotic oxida-
tion (Charrié-Duhaut et al. 2000); although the level of oxida-
tion and biodegradation varies from one site to another. One
highly degraded sample has equal proportions of saturated and
aromatic hydrocarbons, indicating the preferential removal of
aromatics relative to saturated hydrocarbons, which is an ad-
ditional indication of oxidation. The preferential degradation
of aromatics relative to saturated hydrocarbons was also pre-
viously recorded in weathered shales (Clayton and Swetland

1978) and from severely degraded oil spills (Wang et al. 1994;
Charrié-Duhaut et al. 2000). Biodegradation and oxidation
can act with different intensity on the bitumens, so moderate
biodegradation may operate with intense oxidation (Hauck
et al. 2013). The effect of oxidation in the present study sam-
ples is reflected in the hydrogen isotopes as discussed above.

Thermal maturity of bitumen

Alkanes and aromatic biomarkers of oil may be affected by
alteration processes such as biodegradation and water wash-
ing; therefore, the parameters used for the determination of
source, depositional environment and thermal maturity of or-
ganic matter can be problematic (Bennett and Larter 2018).

The Ts/Ts + Tm ratio is widely used as a thermal maturity
indicator, but it should be used with caution because it is
dependent on lithology and biodegradation (Peters et al.
2005). The Ts/Ts + Tm ratio of most of the samples studied
are generally low (less than 0.24; Table 2), indicating a low
thermal maturity level, which is supported by the low values
of C_{29} 20S/20S + 20R steranes (0.19–0.44) and of C_{29} ββ/
αα + ββ (0.16–0.52) steranes for most samples that are
slightly to moderately biodegraded (Table 3). These values
are lower than the equilibrium values (0.67–0.70 for C_{29}
ββ/αα + ββ steranes and 0.52–0.55 for C_{29} 20S/20S + 20R
steranes) and indicate that the source rocks of bitumens have
not reached the peak of their oil window. The C_{32} 22S/22S +
22R hopane ratio has reached the equilibrium value for most
samples (Table 4), indicating that they have reached or passed
the early maturity level. However, this ratio is affected by
biodegradation; therefore, it must be used as maturity param-
eter with caution.

Aromatic biomarkers are also commonly used for the assessment of the thermal maturity level, and these parameters can be used throughout the whole oil window (Luo et al. 2016) when most of the aliphatic parameters reached the equilibrium at early peak of the oil window. Also, aromatic hydrocarbons are more resistant to biodegradation than saturated hydrocarbons and could be used to assess the level of thermal maturity of the biodegraded oils.

The methyldibenzothiophene ratio (MDR) values of the bitumen samples (Table 2) are generally high (between 1.86 and 3.87), which suggest that the source rocks have a high maturity level. However, the bitumen samples of the present study were found to have been affected by water washing (see below), which alters the more soluble aromatic hydrocarbon such as dibenzothiophene.

The triaromatic steroids, which are highly resistant biomarkers, are valid for maturity assessment in these bitumen samples. Their low-cracking ratio (0.01–0.07; Table 2) indicate that they have a low level of maturity.

To summarize, the low thermal maturity of these bitumens is consistent with the assumption that at outcrops they are generally less mature than crude oils that are trapped at depth in well-protected reservoirs (Connan et al. 2013).

Source of organic matter and depositional environment

The biomarkers of saturated and aromatic hydrocarbons used for the depositional environment interpretation of source rocks are listed in Table 2. However, due to the removal of normal alkanes and isoprenoids in all samples, ratios such as Pristane/Phytane, Pristane/n-C_{17} and Phytane/n-C_{18} of the pristine (migrated) bitumen cannot be calculated. In addition, the hopanes and steranes of some samples are degraded and, consequently, the terpane and sterane ratios must be used with caution. Therefore, biomarkers that are more resistant to biodegradation, such as C35 hopane and diasteranes, will be relied upon to interpret the depositional environment and organic matter source. Tricyclic terpanes, which are widely used to infer the lithology of source rocks, are present in a very low concentration, in spite of their resistance to biodegradation, having obviously been removed in the asphalts by water washing.

As mentioned previously, the sulphur content of all samples is very high, suggesting a carbonate depositional environment under anoxic conditions for their source rocks (Tissot and Welte 1984). Sulphur content of the oil seeps from Sierra de Perija, Venezuela, which are likely generated from marine calcareous source rocks, is lower than 6.36 wt.% (Escobar et al. 2011); it is lower than 5 wt.% for the severely biodegraded bitumens from Upper Devonian Carbonates, Canada (Park et al. 2018). Therefore, the very high sulphur content of the present bitumens may suggest that they were generated from type II-S kerogen. Moreover, carbonate source rocks of bitumens are supported by the presence of C_{32}–C_{35} hexahydrobenzohopanes, which are characteristic of oil generated from sulphur-rich carbonate-anhydrite source rocks (Connan and Dessort 1987; Summons et al. 1999). In addition, the C_{35}/C_{34} hopanes ratio is high (more than 1) in seven sandstones (average 1.57), whereas the other two solid bitumens have lower values (less than 1). These high C_{35}/C_{34} values are associated with a relatively high homohopane index for the seven sandstones (more than 0.20, average 0.23) and lower values (0.11; Table 2) in the two solid bitumens. This property suggests that their source rock contained marine organic matter deposited under highly reducing conditions (Peters and Moldowan 1991; Peters et al. 2005). Moreover, the diasteranes/regular steranes ratio is very low (0.09–0.16) except in the two solid bitumens, which have slightly higher values (0.21–0.43; Table 3), which is consistent with a low clay content in the source rocks. The similarity in the triaromatic sterane patterns of the seven sandstones, exemplified by sample Nos. 1 and 2 in Fig. 14, suggests that they have a common origin, whereas the two solid bitumens (Nos. 3 and 4 in Fig. 14), which show different fingerprints, have a different origin (Fig. 14).

In summary, the seven samples (Nos. 1, 2 and 5–9) have a common origin—carbonate source rocks deposited under reducing conditions, whereas the two samples (Nos. 3 and 4) have a different source rock with a clay-rich lithology. The high clay content of the source rocks for these two samples is supported by the higher Ts/Ts + Tm (0.22–0.24) and diasteranes/regular steranes (0.21–0.43) values, but they have a lower $C_{35}S/C_{34}S$ ratio (0.85–0.99) and homohopane index (0.11) than those of the other samples (Tables 2 and 3; Fig. 15), indicating a more oxic environment. These two samples have the lowest sulphur content among the samples (6.6–7.4%; Table 1), which provides further evidence of their source rocks having a clay-rich lithology.

By contrast, the dibenzothiophene/phenanthrene (DBT/P) ratio, low in all samples (less than 0.3; Table 2), may suggest clastic source rocks for these bitumens (Hughes et al. 1995) but no supporting indicators for this assumption were recorded. The low DBT/P ratio could be due to the effect of the alteration process, especially the water-washing process (Palmer 1984). Dibenzothiophene is more water soluble than phenanthrene; therefore, the DBT/P ratio will decrease in oil samples subjected to water washing (Palmer 1984; Hughes et al. 1995). Moreover, the methyldibenzothiophene/methylphenanthrene (MDBT/MP) ratio is well correlated with the DBT/P ratio in the unaltered oils (correlation coefficient 0.92) (Hughes et al. 1995). In the samples of the present study, the MDBT/MP values are not well correlated with the DBT/P values; they are higher (Table 2) because the MDBT and MP are less soluble than DBT and P (Palmer 1984).

Fig. 14 Mass chromatogram of the triaromatic steranes ($m/z =$ 231) of selected bitumen samples (see Table 1 for sample information)
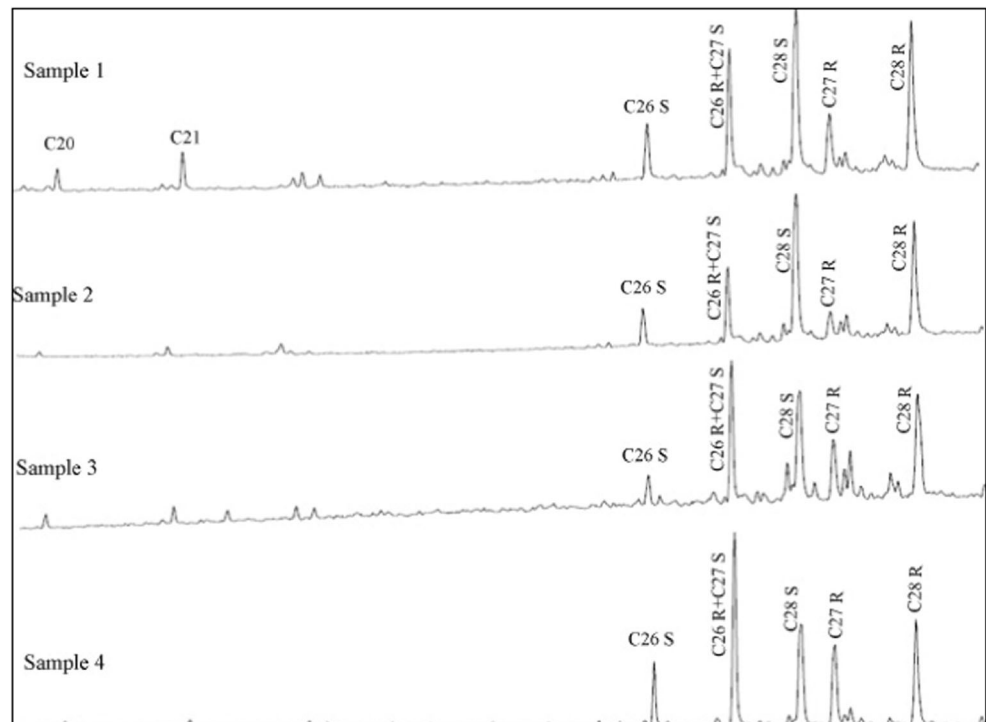
Potential source rock

The genesis of the bitumens from the Kolosh Formation can be ruled out for several reasons. The presence of bitumens in the lower part of Kolosh Formation (especially at Dokan area) indicates they migrated from older formations. The TOC of the Kolosh Formation is about 0.45 wt.% and is early mature source rock in the Taq Taq Oilfield (Baban and Ranyayi 2013). However, in the Bijeel-1 Well, the TOC values are between 1.63 and 5.52 wt.% with HI values between 466 and 676 mg HC/g TOC, and the sediments are immature (Abdula et al. 2017). The Kolosh Formation consists of dominant clastic sediments, as discussed previously, and the
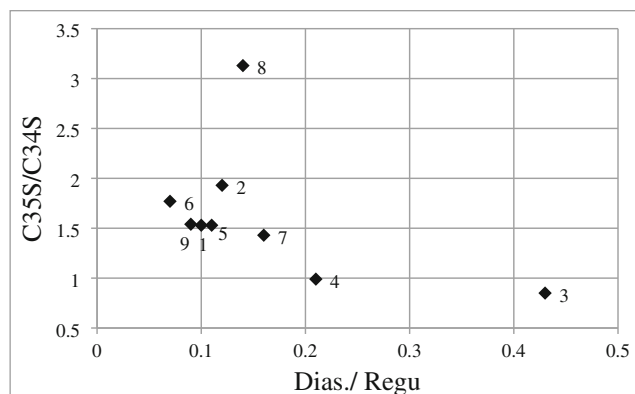
bitumens of that study were generated from carbonate source rocks. The organic matter of the Kolosh Formation is mainly terrestrial (type III) and gas prone in the Taq Taq Oilfield (Baban and Ranyayi 2013) and type II in the Bijeel-1 Well; the studied bitumens are likely to have been generated from type II or type II-S kerogen. Finally, only two bitumens (Nos. 3 and 8), which are heavily biodegraded, show a possible occurrence of 18α (H)-oleanane, which has not been definitely substantiated due to interference with other molecules. However, the presence of 18α(H)–oleanane in these samples could be due to contamination during migration through Cretaceous–Tertiary successions and to its greater resistance to biodegradation. Its concentration significantly increases in the heavily biodegraded samples while its absence in other samples indicates that the source rock is older than Tertiary. The Kolosh Formation, which is Palaeocene, has to be ruled out.

In Iraq, source rocks were recognized from Palaeozoic to Tertiary. Silurian hot shale of Akkas Formation is the main Palaeozoic source rock in Iraq (Aqrawi 1998; Al-Hadidy 2007; Alkhafaji et al. 2015), but the most important source rocks for oil are the Jurassic–Lower Cretaceous formations, represented by Sargelu, Naokalekan and Chia Gara Formations. Other secondary source rocks include Triassic Kurra Chine, Cretaceous Gulneri, Sulaiy and Balambo Formations. The regular $\beta\beta$ sterane distribution of sample No. 4 is not affected by biodegradation and is similar to that of the oil sample from the Shorish-1 Well (about 35 km southwest of Shaqlawa; Fig. 16), which was generated by

Fig. 15 The relationship between the C_{35}/C_{34} hopanes versus the diasteranes/regular steranes of the bitumen samples (see Table 1 for sample information)

Cretaceous and Jurassic units represented by the Sargelu (Middle Jurassic), Naokelekan (Upper Jurassic) and/or Chia Gara (Upper Jurassic–Lower Cretaceous) Formations (Sachsenhoger et al. 2015). The regular sterane distribution of sample No. 4 is similar to that of Tawke oil and seepage, which is located near Zakho in northern Iraq (Fig. 16). This oil and asphalt was generated from Lower–Middle Jurassic source rocks (Abdula 2017). The main difference between the Tawke seepage and the bitumens of the present study is that the former is mature (Connan et al. 2013; Abdula 2017) and those of the present study are early mature. The sulphur content of Tawke oil is also high (more than 3.1 wt.%; Abdula 2015). The gammacerane index value of the biodegraded oil of the Cretaceous units from the Shorish-1 Well (northern Iraq) is between 0.15 and 0.17 (Sachsenhoger et al. 2015), which are very close to those of the moderately biodegraded samples of the present study (Group 1 samples), which ranges between 0.17 and 0.20. The carbon isotopes values of the aromatic fraction of the samples from the present study are very close to those of the Sargelu Formation extract recorded by Abdula (2015) which range between −28.08 and −26.91 ‰. The polar fraction comprises more than 90% of the rock sample extract of the Sargelu Formation in the Duhok area (Abdula 2015), which is very close to the values of the present study samples. The carbon isotopes of asphaltene of the present study also exhibit values close to those of the bitumen seeps of Qaiyarah, Fat'ha, Hammam Al-Alil and Mishraq in northern Iraq (Connan et al. 2013; Fig. 8). In addition, the terpane biomarkers and the presence of hexahydrobenzohopanes in the bitumen samples indicate that these bitumens were generated from sulphur-rich carbonate source rocks. This could indicate that the bitumens of the present study were generated from the Sargelu, Naokelekan and Chia Gara Formations, which were considered the main source rocks for oil in Iraq and their equivalents in Iran (Aqrawi et al. 2010; Al-Ameri and Zumberge 2012; Connan 2012). The first two formations consist of interlayered shale and bituminous limestone and contain type II-S kerogen (Pitman et al. 2003), whereas the Chia Gara Formation is dominated by radiolarian limestone and dark calcareous shale, and also contain type II-S kerogen (Hakimi et al. 2018). These formations were generating hydrocarbons with high sulphur content at low maturities (Sachsenhoger et al. 2015). Thermal maturity of Sargelu Formation, which is the main Jurassic source rocks, increases northeastward (Abdula 2015). In the Taq Taq and Kirkuk oilfields, the main phase of hydrocarbon generation occurred during Neogene (Pitman et al. 2004), whereas Sachsenhoger et al. (2015) suggested two peaks for oil generation from the Sargelu, Naokelekan and Chia Gara Formations at the Shorish-1 Well, the first being Palaeocene/Eocene and the second Late Miocene/Pliocene. In addition, the presence of these bitumens in the Palaeocene Kolosh Formation and their absence in the overlying Eocene Formations (Gercus or Sinjar) indicate that migration of these

Fig. 16 Ternary diagram of the regular sterane distribution in the bitumen and oil samples (see Table 1 for sample information)
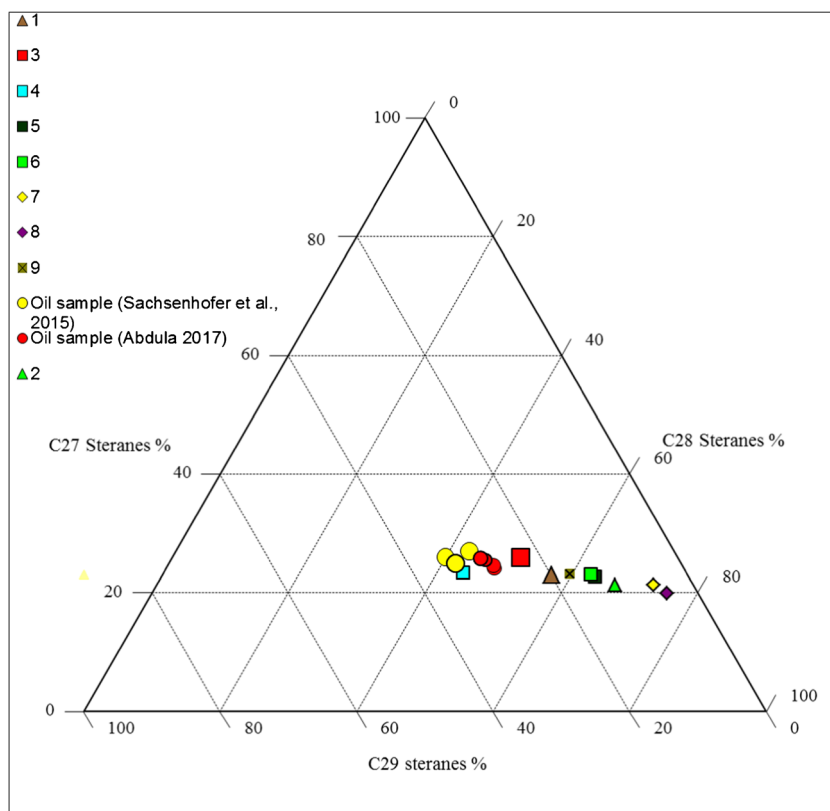
oils to Kolosh Formation took place before deposition of the Eocene Formations, consistent with the first peak of oil generation for Sargelu, Naokelekan and Chia Gara Formations as suggested by Sachsenhoger et al. (2015).

Solid bitumens fill fractures in sandstones or wrap the sandstone balls in a thin crust (Figs. 2 and 3). These sandstone balls were formed as deformational structures after lithification of the sands during burial and subsequent uplifting (Karim 2005), suggesting that the migration of solid bitumens took place after the deposition and lithification of the Kolosh Formation (i.e. after the Palaeocene–Eocene).

Migration of oil from Jurassic and Cretaceous source rocks, or from palaeotraps to Cenozoic reservoirs took place along vertical pathways (Aqrawi et al. 2010). Palaeotrap seal rocks were fractured due to tectonic movement during Zagros deformation, which led to an upward migration of the underlying Jurassic and Cretaceous oils. Pitman et al. (2004) estimated that approximately 1500 and 2000 m of the Neogene uplift entailed erosion in Zagros area and Thrust zones, respectively, which led to seal failure and the degassing of oil (Aqrawi et al. 2010), leaving heavy oil, such as that of the present study, especially at the Duhok site, which is a characteristic oil trap composed of porous, coarse sandstone.

The bituminous sandstone bed is restricted to the upper part of the formation at Duhok and Shaqlawa and to the lower part at Dokan, whereas the solid bitumen is distributed in the middle and upper parts at Shaqlawa and Dokan. The age biomarkers (aromatic dinosteroid ratio) are similar among all samples (Table 2), indicating that the source rocks of the bitumen samples are the same age, in spite of their differing lithologies.

Conclusions

The study of the bitumens of the Kolosh Formation in northern Iraq led to the following conclusions:

1. These bitumens are biodegraded to different extents. Group 1 samples are moderately biodegraded (levels 5–6 of Peter and Moldowan) with normal alkanes and isoprenoids completely removed, whereas the steranes and hopanes are intact. Group 2 samples are heavily to very heavily biodegraded (levels 7–8 of Peter and Moldowan) with partially degraded hopanes and steranes; these samples were also subjected to abiotic oxidation to different extents.

2. These bitumens were generated from early mature organic matter and have different origins, but all were generated from carbonate source rocks. The samples from bituminous sandstone were generated from clay-poor carbonate source rocks deposited under reducing conditions, whereas the two solid bitumens were generated from clay-rich

carbonate source rocks deposited under more oxic conditions.

3. The most likely candidate for the source rocks of these bitumens is from Jurassic and Upper Jurassic–Lower Cretaceous formations, represented by the Sargelu, Naokelekan and Chia Gara Formations.

4. There are two phases of bitumen migration: the first represents bituminous sandstone and the second solid bitumen.

Compliance with ethical standards

References

Abdula RA (2015) Hydrocarbon potential of Sargelu Formation and oil-source correlation, Iraqi Kurdistan. Arab J Geosci 8:5845–5868

Abdula RA (2017) Geochemistry links source rocks, crude distribution in northern Mesopotamian Basin, Iraq. Oil Gas J 115:38–50

Abdula RA, Ali MA, Ahmed MM, Hamad HR (2017) Rock-Eval pyrolysis results from the Bijeel 1 well, Kurdistan Region, Iraq. ZANCO Journal of Pure and Applied Sciences 29:29–38

Al-Ameri TK, Zumberge J (2012) Middle and Upper Jurassic hydrocarbon potential of the Zagros Fold Belt, North Iraq. Mar Pet Geol 36:13–34

Al-Hadidy AH (2007) Paleozoic stratigraphic lexicon and hydrocarbon habitat of Iraq. GeoArabia 12:63–130

Alkhafaji MW, Aljubouri ZA, Aldobouni IA, Littke R (2015) Hydrocarbon potential of Ordovician–Silurian successions in Akkas Field, Western Desert of Iraq. Am Assoc Pet Geol Bull 99:617–637

Aqrawi AAM (1998) Paleozoic stratigraphy and petroleum systems of the Western and Southwestern Desert of Iraq. GeoArabia 3:229–248

Aqrawi AAM, Goff JC, Horbury AD, Sadooni FN (2010) The petroleum geology of Iraq: Beaconsfield. Scientific Press Ltd, United Kingdom, p 423

Asif M, Grice K, Fazeelat T (2009) Assessment of petroleum biodegradation using stable hydrogen isotopes of individual saturated hydrocarbon and polycyclic aromatic hydrocarbon distributions in oils from the Upper Indus Basin, Pakistan. Org Geochem 40:301–311

Baban DH, Ranyayi KSM (2013) Potentiality of Palaeocene source rocks and their contribution in generation the accumulated oil in the Eocene PilaSpi Reservoir in Taq Taq oil field, Kurdistan Region, Iraq. Arab J Geosci 6:4225–4237

Bennett B, Larter SR (2018) Geological controls on the heterogeneous hydrocarbon compositions of the biodegraded Grosmont Formation bitumen, Western Canada Sedimentary Basin. Org Geochem 125:243–259

Bennett B, Fustic M, Farrimond P, Huang H, Larter SR (2006) 25-Norhopanes: formation during biodegradation of petroleum in the subsurface. Org Geochem 37:787–797

Blanc P, Connan J (1992) Origin and occurrence of 25-norhopanes: a statistical study. Org Geochem 18:813–828

Bost FD, Frontera-Suau R, McDonald TJ, Peters KE, Morris PJ (2001) Aerobic biodegradation of hopanes and norhopanes in Venezuelan crude oils. Org Geochem 32:105–114

Charrié-Duhaut A, Lemoine S, Adam P, Connan J, Albrecht P (2000) Abiotic oxidation of petroleum bitumens under natural conditions. Org Geochem 31:977–1003

Chosson P, Connan J, Dessort D, Lanau C (1992) In vitro biodegradation of steranes and terpanes: a clue to understanding geological situations. In: Moldowan JM, Albrecht P, Philp RP (eds) Biological markers in sediments and petroleum. Prentice-Hall, Englewood Cliffs, pp 320–349

Clayton JL, Swetland PJ (1978) Subaerial weathering of sedimentary organic matter. Geochim Cosmochim Acta 42:305–312

Connan J (1984) Biodegradation of crude oil in reservoirs. In: Welte H (ed) Brooks, J, vol 1. Academic Press, London, pp 299–335

Connan J (1999) Use and trade of bitumen in antiquity and prehistory: molecular archaeology reveals secrets of past civilizations. Phil Trans R Soc Lond B 354:33–50

Connan J (2012) Le bitume dans l'antiquité. Editions Errance, Arles, 269 pages

Connan J, Dessort D (1987) Novel family of hexacyclic hopanoid alkanes (C_{32}–C_{35}) occurring in sediments and oils from anoxic palaeoenvironments. Org Geochem 12:103–113

Connan J, Kozbe G, Kavak O, Zumberge J, Imbus K (2013) The bituminous mixtures of Kavuşan Höyük (SE Turkey) from the end of the 3rd millennium (2000 BC) to the Medieval period (AD 14th century): composition and origin. Org Geochem 54:2–18

da Cruz GF, Neto VDS, Marsaioli AJ (2008) Petroleum degradation by aerobic microbiota from the Pampo Sul Oil Field, Campos Basin, Brazil. Org Geochem 39:1204–1209

Escobar M, Marquez G, Inciarte S, Rojas J, Esteves I, Malandrino G (2011) The organic geochemistry of oil seeps from the Sierra de Perija eastern foothills, Lake Maracaibo Basin, Venezuela. Org Geochem 42:727–738

Frontera-Suau R, Bost FD, McDonald TJ, Morris PJ (2002) Aerobic biodegradation of hopanes and other biomarkers by crude oil-degrading enrichment cultures. Environ Sci Technol 36:4585–4592

Goodwin NS, Park PJD, Rawlinson AP (1983) Crude oil biodegradation under simulated and natural conditions. In: Bjorøy M et al (eds) Advances in organic geochemistry. J. Wiley and Sons, New York, pp 650–658

Hakimi MH, Mohialdeen MJ, Al Ahmed AA, El Nady M (2018) Thermal modelling and hydrocarbon generation of the Late Jurassic-Early Cretaceous Chia Gara Formation in Iraqi Kurdstan Region, northern Zagros Fold Belt. Egypt J Pet 27:701–713

Hauck TC, Connan J, Charrié-Duhaut A, Tensorer J-ML, al Sakhel H (2013) Molecular evidence of bitumen in the Mousterian lithic assemblage of Hummal (Central Syria). J Archaeol Sci 40:1–11

Hosseini SH, Horsfield B, Wilkes H, Vieth-Hillebrand A, Yalcin MN, Kavak O (2018) Comprehensive geochemical correlation between surface and subsurface hydrocarbon occurrences in the Batman-Mardin-Sirnak area (SE Turkey). Mar Pet Geol 93:95–112

Hughes WB, Holba AG, Dzou LIP (1995) The ratios of dibenzothiophene to phenanthrene and pristane to phytane as indicators of depositional environment and lithology of petroleum source rocks. Geochim Cosmochim Acta 59:3581–3598

Jassim SZ, Buday T (2006a) Middle Palaeocene–Eocene Megasequence (AP10). In: Jassim SZ, Goff JC (eds) Geology of Iraq. Prague and Moravian Museum, Brno, pp 117–123

Jassim SZ, Buday T (2006b) Tectonic framework. In: Jassim SZ, Goff JC (eds) Geology of Iraq. Brno, Prague and Moravian Museum, pp 45–56

Karim KH (2005) Origin of ball and pillow-like structures in Tanjero and Kolosh Formations in Sulaimaniya area, NE-Iraq. Kurdistan Academicians Journal 4:1–9

Lafargue E, Barker C (1988) Effect of water washing on crude oil compositions. AAPG Bull 72:263–276

Larter S, Wilhelms A, Head I, Koopmans M, Aplin A, Di Primio R, Zwach C, Erdmann M, Telnaes N (2003) The controls on the composition of biodegraded oils in the deep subsurface: part I—biodegradation rates in petroleum reservoirs. Org Geochem 34:601–613

Larter S, Huang H, Adams J, Bennett B, Jokanola O, Oldenburg T, Jones M, Head I, Riediger C, Fowler M (2006) The controls on the composition of biodegraded oil in the deep surface: part II—geological controls on subsurface biodegradation fluxes and constraints on reservoir-fluid property prediction. AAPG Bull 90:921–938

Larter S, Huang H, Adams J, Bennett B, Snowdon LR (2012) A practical biodegradation scale for use in reservoir geochemical studies of biodegraded oils. Org Geochem 45:66–76

Lin HH, Michael GE, Kovachev G, Zhu H, Philp RP, Lewis CA (1989) Biodegradation of tar-sand bitumens from the Ardmore and Anadarko Basins, Carter County, Oklahoma. Org Geochem 14:511–523

Lopez L, Monaco SL, Volkman JK (2015) Evidence for mixed and biodegraded crude oils in the Socororo field, Eastern Venezuela Basin. Org Geochem 82:12–21

Luo Q, George SC, Xu Y, Zhong N (2016) Organic geochemical characteristics of the Mesoproterozoic Hongshuizhuang Formation from Northern China: implications from thermal maturity and biological sources. Org Geochem 99:23–37

Moldowan JM, Lee CY, Sundararaman P, Salvatori T, Alajbeg A, Gjukic B, Demaison GJ, Slougui N, Watt DS (1992) Source correlation and maturity assessment of select oils and rocks from the central Adriatic Basin (Italy and Yugoslavia). In: Moldowan JM, Albrecht P, Philp RP (eds) Biological markers in sediments and petroleum. Prentice-Hall, New Jersey, pp 370–401

Moldowan JM, Dahl J, McCaffrey MA, Smith WJ, Fetzer JC (1995) Application of biological marker technology to bioremediation of refinery by-products. Energy and Fuels 9:155–162

Numan NMS (1997) A plate tectonic scenario for the Phanerozoic succession in Iraq. Iraqi Geological Journal 30:85–119

Orr WL (1978) Sulfur in heavy oils sands and oil shale. In: Strausz OP, Lown EM (eds) Oil sand and oil shale chemistry. Verlag Chemie International, New York, pp 223–243

Palmer SE (1984) Effect of water washing on C15+ hydrocarbon fraction of crude oils from northwest Palawan, Philippines. AAPG Bull 8:137–149

Park MH, Kil Y, Choi J, Seol J, Kim JH (2018) Biodegradation characteristics of bitumen from the Upper Devonian carbonates (Grosmont and Nisku formations) in Alberta, Canada. Geosci J 1–11

Peters K, Moldowan JM (1991) Effects of source, thermal maturity and biodegradation on the distribution and isomerization of homohopanes in petroleum. Org Geochem 17:47–61

Peters KE, Moldowan JM (1993) The biomarker guide. Interpreting molecular fossils in petroleum and ancient sediments. Prentice Hall, Englewood Cliffs, New Jersey, p 363

Peters KE, Moldowan JM, McCaffrey MA, Fago FJ (1996) Selective biodegradation of extended hopanes to 25-norhopanes in petroleum reservoirs. Insights from molecular mechanics. Org Geochem 24: 765–783

Peters KE, Walters CC, Moldowan JM (2005) The biomarker guide, 2nd edn. Cambridge University Press, Cambridge, p 1155

Pitman JK, Steinshouer DW, Lewan MD (2003) Generation and migration of petroleum in Iraq, a 21/2D and 3D modelling study of Jurassic source rocks: AAPG international meeting in Cairo, Egypt, compiled power point slides, open-file report 03–192

Pitman JK, Steinshour D, Lewan MD (2004) Petroleum generation and migration in the Mesopotamian Basin and Zagros Fold Belt of Iraq, result from a basin modeling study. GeoArabia 9:41–72

Requejo AG, Halpern HI (1989) An unusual hopane biodegradation sequence in tar sands from the Pt Arena (Monterey) Formation. Nature 342:70–673

Rubinstein I, Strausz OP, Spyckerelle C, Crawford RJ, Westlake DWS (1977) The origin of the oil sand bitumen of Alberta: a chemical and microbiological simulation study. Geochim Cosmochim Acta 41: 1341–1353

Sachsenhoger RF, Bechtel A, Gratzer R, Rainer TM (2015) Source-rock maturity, hydrocarbon potential and oil-source-rock correlation in well Shorish-1, Erbil Province, Kurdistan region, Iraq. J Pet Geol 38:357–382

Seifert WK, Moldowan JM (1979) The effect of biodegradation on steranes and terpanes in crude oils. Geochim Cosmochim Acta 43: 111–126

Seifert WK, Moldowan JM, Demaison GJ (1984) Source correlation of biodegraded oils. Org Geochem 6:633–643

Stern B, Connan J, Blakelock E, Jackman R, Coningham RAE, Heron C (2008) From Susa to Anuradhapura: reconstructing aspects of trade and exchange in bitumen-coated ceramic vessels between Iran and Sri Lanka from the Third to the Ninth centuries AD. Archaeometry 50:409–428

Summons RE, Jahnke LL, Hope JM (1999) 2-Methylhopanoids as biomarkers for cyanobacterial oxygenic photosynthesis. Nature 400: 554–557

Sun Y, Chen Z, Xu S, Cai P (2005) Stable carbon and hydrogen isotopic fractionation of individual alkanes accompanying biodegradation: evidence from a group of progressively biodegraded oils. Org Geochem 36:225–238

Tissot BP, Welte DH (1984) Petroleum formation and occurrence, 2nd edn. Springer-Verlag, New York, p 699

Volkman JK, Alexander B, Kagi RI, Woodhouse GW (1983) Demethylated hopanes in crude oils and their application in petroleum geochemistry. Geochim Cosmochim Acta 47:785–794

Volkman JK, Alexander R, Kagi RI, Rowland SF, Sheppard PN (1984) Biodegradation of aromatic hydrocarbons in crude oils from the Barrow Sub-basin of Western Australia. Org Geochem 6:619–632

Wang Z, Fingas M, Sergy G (1994) Study of 22-year-old Arrow oil samples using biomarker compounds by GC/MS. Environ Sci Technol 28:1733–1746

Wang G, Xue Y, Wang D, Shi S, Grice K, Greenwood PF (2016) Biodegradation and water washing within a series of petroleum reservoirs of the Panyu Oil Field. Org Geochem 96:65–5476

Watson JS, Jones DM, Swannell RPJ, Duin ACT (2002) Formation of carboxylic acids during aerobic biodegradation of crude oil and evidence of microbial oxidation of hopanes. Org Geochem 33: 1153–1169

Wenger LM, Isaksen GH (2002) Control of hydrocarbon seepage intensity on level of biodegradation in sea bottom sediments. Org Geochem 33:1277–1292